Appl. Phys. B 56, 249–258 (1993)

Applied Physics B Photophysics and Laser Chemistry

State-to-State Rotational Energy Transfer in OH ($A^2\Sigma^+$, $v' = 1$)

R. Kienle, A. Jörg*, K. Kohse-Höinghaus

DLR-Institut für Physikalische Chemie der Verbrennung, Pfaffenwaldring 38–40, W-7000 Stuttgart 80, Germany
(Fax: +49-711/6862-349)

Received 18 December 1992/Accepted 22 February 1993

Abstract. State-to-state rotational energy transfer (RET) coefficients for thermal collisions of OH ($A^2\Sigma^+$, $v' = 1$) with He, Ar, N_2, CO_2, and H_2O at 300 K were determined from time-resolved laser-induced fluorescence (LIF) measurements. The RET coefficients are very similar in both qualitative behaviour and absolute magnitude to those measured previously for OH ($A^2\Sigma^+$, $v' = 0$).

PACS: 34.00

The detection of reactive species is an important aspect of combustion diagnostics. Knowledge of radical concentration distributions provides valuable clues for characterization of the combustion process as well as for identification of reaction pathways which may lead to undesired or chemically hazardous products. Laser-induced fluorescence is one of the most versatile techniques suitable to measure the concentrations of reactive intermediates – often in conjunction with temperature – in combustion systems. However, it is well-known that the influence of collision processes on fluorescence spectrum and intensity may render a quantitative interpretation of LIF signals difficult. In general, detailed information on the efficiency of collisional energy transfer and its dependence on temperature and chemical environment is required for accurate measurements of temperature and concentration. Even though several variants of the LIF technique are sufficiently insensitive to collisions for many combustion situations, none of them is generally applicable.

Instead of relying on one specific LIF approach, we have thus adopted a slightly different philosophy: with the aid of a detailed dynamic model, we attempt to examine the specific influences of collision processes on the fluorescence signals *before* the actual experiment in order to identify the optimal experimental procedure. We have begun to assemble such a numeric model for the OH radical which simulates all radiative and collisional processes of relevance with the appropriate system of differential equations. OH was chosen for obvious reasons: it is a molecule of key importance in combustion systems, and a significant amount of data on collisional energy transfer is already available. Apart from the radiative transfer rates, the modelling requires information on electronic quenching as well as on vibrational and rotational energy transfer (VET and RET, respectively) for a large temperature range and for various collision partners.

This article is part of a series in which we describe the model and provide some of the necessary rate coefficients. We have begun with the investigation of rotational energy transfer in the electronically excited ($A^2\Sigma^+$) state of the OH radical. For this, we have developed a method which allows the direct determination of the state-to-state RET coefficients from time-resolved fluorescence measurements [1, 2]. The method was first applied to measure RET coefficients for thermal collisions of OH ($A^2\Sigma^+$, $v' = 0$) with He and Ar at room temperature [1]. In parallel with this experimental investigation, ab initio calculations were performed for the RET of OH (A, $v' = 0$) with both collision partners [3–5]. Very good agreement between our experimental results and those of the theoretical studies was observed. In a next step, we measured state-to-state RET coefficients at 300 K for collisions of OH (A, $v' = 0$) with some combustion-relevant colliders, namely N_2, CO_2 and H_2O [6]. The present article reports on an analogous study of RET in the vibrationally excited OH (A, $v' = 1$) state at 300 K with the collision partners He, Ar, N_2, CO_2, and H_2O. For the measurement of OH concentrations or temperature in combustion systems with large OH mole fractions, excitation to $v' = 1$ – typically via the (A–X, 1,0) transition – is often more favourable than the alternative (A–X, 0,0) excitation: absorption of the laser radiation by OH in the flame can be significantly reduced due to the smaller Franck-Condon factor for the (1,0) transition. In addition, an idea of the dependence of the RET on vibrational level for a number of differently structured collision partners can be gained by comparison of the data reported previously [6] with those measured in the present study, thus providing vital information for a realistic representation of rotational energy transfer in a dynamic LIF model.

* Now with IBM Frankfurt, Germany

The article is organized in the following way. Section 1 describes the experimental setup, followed by a discussion in Sect. 2 of the experimental method and the data evaluation procedure. For example, the influence of vibrational energy transfer (VET) on the accurate determination of RET coefficients is examined in Sect. 2. Results are reported and discussion in Sect. 3. The paper concludes with a detailed analysis of potential sources for statistical and systematic errors in Sect. 4.

1 Experiment

The experimental arrangement was largely the same as described previously [1, 6]. We used a laser system consisting of a Nd:YAG laser (Spectra Physics DCR-2), a dye laser (PDL-2, Rhodamine 6G) and a frequency doubler (WEX). The $R_2(4)$ line [1] in the OH ($A^2\Sigma^+ - X^2\Pi, 1, 0$) transition near 281.76 nm was excited. At typical operation conditions, the pulse energy was in the range of 8–15 mJ (≈10 mJ for most experiments), the pulse duration was ≈6 ns FWHM, and the laser bandwidth was ≈2 cm^{-1} FWHM (which is much larger than the Doppler width of 0.1 cm^{-1} at 3400 K). The laser beam was weakly focussed to a diameter of ≈3–4 mm. A polarization scrambler was used to destroy any orientational preference in the excitation process.

OH was produced in a discharge flow reactor at 300 K and at pressures of a few mbar by the reaction of H atoms with NO_2. Hydrogen atoms were generated in a flow of a small amount of H_2 in Helium. Typical flow reactor conditions including the mole fractions of the different collision partners are given in Table 1. RET by He was measured without addition of any collider flow whereas Ar, N_2, CO_2, or H_2O were added to the background mixture of He, H_2, and NO_2. All flows except that of H_2O were determined with mass flow controllers (Tylan FC 280S); the H_2O flow was measured with a mass flow meter (Hastings EALL 500).

The fluorescence was measured using two separate detection channels with different spectral bandpasses: a narrow-band system for the actual RET measurements and a broad-band reference system which monitored changes in the operating conditions of the laser or the flow reactor. In the former system, which was used to detect isolated fluorescence lines in the (1, 1) band, the fluorescence light was collected with two lenses of $f = 150$ mm and $f = 200$ mm and imaged onto the (vertical) slit of a 0.64 m monochromator (Jobin Yvon HR 640) after rotation of the image by a two-mirror combination. In most experiments, slit width and height were 50 μm and 2 mm, respectively, yielding a spectral resolution of ≈4 cm^{-1}. (For some measurements where this resolution was not necessary, width and height were increased to 100 μm and 5 mm, respectively, to increase the signal-to-noise ratio.) The time-resolved fluorescence signal was detected with a XP 2020Q photomultiplier (Valvo) and recorded with a 400 MHz transient digitizer (Tektronix 7912 AD). Typically, the first 100 or 200 ns of the fluorescence signals were recorded, depending on pressure and collision partner. Calibrated neutral density filters were used to attenuate the fluorescence signal if necessary.

The broad-band reference signal is proportional to the total number density of excited OH. Thus, it was used to indicate changes in OH production or in laser intensity and wavelength. The fluorescence was detected with a second XP 2020Q photomultiplier and recorded with a boxcar integrator (Stanford Research Systems SRS 250). Scattered laser light was suppressed by a filter combination of UG 11 and WG 320 (Schott) and, in addition, by temporally delaying the boxcar gate. Results of experiments which showed a variation in the reference signal of more than 10% were discarded.

2 Procedure of Measurement and Data Evaluation

2.1 Excitation and Detection Scheme

For the determination of all RET coefficients [2] measured in this work, the $F_2(5)$ level of the OH ($A^2\Sigma^+$, $v' = 1$) state was excited using the $R_2(4)$ transition in the (1, 0) band. Time-resolved single-line fluorescence was observed in the (1, 1) band. Nine state-to-state RET coefficients for inelastic energy transfer out of the excited $F_2(5)$ level to rotational states with the quantum numbers $2 \leq N' \leq 6$ were measured for the collision partners He, Ar and H_2O; four with conserved symmetry [3] ($F_2 \rightarrow F_2$) and five with changing symmetry ($F_2 \rightarrow F_1$). For N_2 and CO_2 as collision partners the coefficients for rotational transfer to the $F_1(2)$ and $F_2(2)$ states could not be measured, due to the fast VET caused by these species [11, 13] leading to interferences with lines in the (0, 0) band.

For all lines, the time-resolved fluorescence signals were monitored at experimentally determined line center positions, thus correcting for slight day-to-day drifts of the

[1] The notation of Dieke and Crosswhite [7] is followed throughout this article

[2] In this work, the term "rotational energy transfer (RET)" refers to collision processes within one vibrational level of a specific electronic state which are inelastic with respect to a rotational quantum number and /or fine structure level

[3] In this context, we refer to e/f symmetry according to Alexander et al. [8]

Table 1. Typical flow reactor conditions for the measurement of RET coefficients: total flow V [sccm], mole fractions χ [%] and pressure p [mbar]

	Collider				
	He	Ar	N_2	CO_2	H_2O
V	2000	2000	1500	1300	1300
$\chi_{collider}$	98	94.5	≈ 58	≈ 64	≈ 30
χ_{He}	–	3.8	≈ 39	≈ 33	≈ 66
χ_{H_2}	1.5	1.5	2.4	2.4	3.3
χ_{NO_2}	0.2	0.2	0.3	0.3	0.8
p	2.0–7.7	1.1–4.0	1.5–3.6	1.5–4.1	0.8–3.0

monochromator wavelength calibration. The line positions were identified before each series of RET experiments by taking OH (1, 1) band fluorescence spectra in a buffer gas of 3–5 mbar Ar, using a gate interval of 0–400 ns. Argon was chosen for this measurement because the RET by Ar shows not preference for symmetry conservation, as will be shown later. For lines that were blended by their satellites we could thus assume a statistical distribution of the populations in both fine structure components.

With our spectral resolution of $\approx 4\,\mathrm{cm}^{-1}$ (slit of 50 µm/2 mm), the following lines in the (1, 1) band were completely isolated and gave access to the corresponding populations in the levels indicated in square brackets: $R_2(5)$ [$F_2(6)$], $P_1(6)$ [$F_1(5)$], $R_2(4)$ [$F_2(5)$], $P_1(5)$ [$F_1(4)$], $O_2(5)$ [$F_1(3)$], and $R_2(1)$ [$F_2(2)$]. Information on the populations in the $F_1(6)$, $F_2(4)$, $F_2(3)$, and $F_1(2)$ levels were obtained from the following line/satellite combinations: $Q_1(6, 6')$, $P_2(5, 5')$, $P_2(4, 4')$, and $Q_1(2, 2')$, respectively. In these cases, the populations could be determined by subtraction as described in [6]. For instance, the time-dependent population of the $F_1(6)$ level could be evaluated from the time-resolved fluorescence signals of the combined $Q_1(6, 6')$ structure and the isolated $R_2(5)$ line: the intensity of the $Q_1(6')$ satellite line was calculated from the measured fluorescence intensity of the $R_2(5)$ line using the appropriate Einstein A coefficients [9] and then subtracted from the measured intensity of the $Q_1(6, 6')$ combination to yield the intensity of the $Q_1(6)$ line. Since the spectral separation of the lines and their satellites are non-negligible ($\geq 1\,\mathrm{cm}^{-1}$ for $N' \geq 5$), the line positions of both components of the spectral structures could not be assumed as coincident for this subtraction. Weight factors which considered the spectral bandpass for each of these line/satellite combinations were therefore determined; they were obtained from a numerical simulation of the spectra with Ar which were taken before in order to measure the line-center positions.

The intensity ratio of line versus satellite is, of course, a function of the degree of symmetry conservation observed for a specific collider. For Ar, N_2 and CO_2, the contribution of the satellite is 10–30% of the total fluorescence intensity. For He and H_2O, which both show a propensity for symmetry conservation (as will be described further below) the situation is different. For the $P_2(N, N')$ structures, the F_2 component is then dominant; only a small fraction of the fluorescence intensity ($\leq$10%) corresponds to the satellite line originating from the F_1 level. The opposite behaviour is observed for $Q_1(N, N')$ detection: in this case, a comparatively large fraction of the fluorescence intensity (of the order of 0.5) has to be subtracted in the data evaluation. The RET coefficients for $F_2(5) \rightarrow F_1(6)$ and $F_2(5) \rightarrow F_1(2)$ transfer by He and H_2O are therefore the ones that may be most affected by errors [4] in the subtraction procedure.

2.2 *Influence of Vibrational Energy Transfer*

The RET coefficients k_{if} for transfer from an initial, laser-excited state i to a final, collisionally populated state f were determined using the formalism of Jörg et al. [1, 2]. The two most relevant equations are repeated here. Equation (1) describes the time-dependent behaviour of the collisionally populated level

$$\frac{dN_f}{dt} = N_c N_i k_{if}^s - \frac{N_f}{\tau_f} . \tag{1}$$

N_i and N_f are the populations in levels i and f, respectively, N_c is the number density of the collider and τ_f is the state-specific natural lifetime. k_{if}^s is the RET coefficient which is derived under the single-collision assumption for the transfer from i to f. Under our experimental conditions, the RET coefficient k_{if}^s is, however, time-dependent due to the increasing probability of multiple collisions with increasing time. The true RET coefficient k_{if} is therefore determined at infinitely low collision probability; this is done by extrapolation of k_{if}^s to $t = t_0$, the start of the laser pulse

$$k_{if} = \lim_{t \rightarrow t_0} k_{if}^s . \tag{2}$$

At low pressures or short observation times, the dependence of k_{if}^s on time t can be approximated by a linear function, the intercept of which yields k_{if} (for details, see model calculations and Fig. 3 in [1]).

The data evaluation procedure described above was successfully applied to measurements in the (0, 0) band [1, 2, 6]. Vibrational energy transfer (VET) was negligible in this case and was thus not included in the differential equations of Jörg et al. [1, 2]. In the present study were $v' = 1$ is excited, VET can no longer be neglected. It will, however, be demonstrated that the same data evaluation procedure as before is valid in this case, without any changes in the pertinent equations.

The influence of vibrational energy transfer on the determination of RET coefficients is illustrated by a numerical simulation of the RET behaviour under conditions which approximately correspond to a realistic experimental situation. We assumed excitation of the OH (A, $v' = 1$) $F_2(5)$ state for N_2 as collision partner at 0.75 mbar and 300 K. It is well known that N_2 causes remarkably fast VET in OH ($A^2\Sigma^+$) [11, 13]. Energy transfer was simulated with or without VET. As an example, the results for transfer to $F_1(4)$ are shown in Fig. 1. For this model calculation the differential equations for 21 rotational/fine structure levels in ($A^2\Sigma^+$, $v' = 1$), for one level representing the ($A^2\Sigma^+$, $v' = 0$) state and for two levels in the ground electronic state (one bath level and one laser-coupled level) were solved. The equations describing the populations in the (A, $v' = 1$) state included terms for the collisional depopulation by VET. The essential parameters for the simulation are listed in Table 2. Radiative rates were taken from Hogan and Davis [12] (in accord with those reported more recently by Burris et al. [13]), rate coefficients for quenching and VET from Burris et al. [13]. Rotational energy transfer was modelled on the basis of our measured RET coefficients as represented by an Energy Corrected Sudden (ECS) scaling law. Our approach [5] is an adaptation of the Infinite Order Sudden (IOS) formalism for RET in $^2\Sigma^+$ states (introduced by Alexander [14]) to the present problem.

The temporal evolution of the populations in the initial ($v' = 1$) $F_2(5)$ state and in the ($v' = 1$) $F_1(4)$ level popu-

[4] For a detailed error analysis, we refer to Sect. 4. ECS and IOS are usually abbreviated this way, so that a capitalized version seems much more appropriate to us (directly shows the reader which law is referred to here

[5] A description of this approach in full detail is beyond the scope of this paper and will be discussed in a future publication

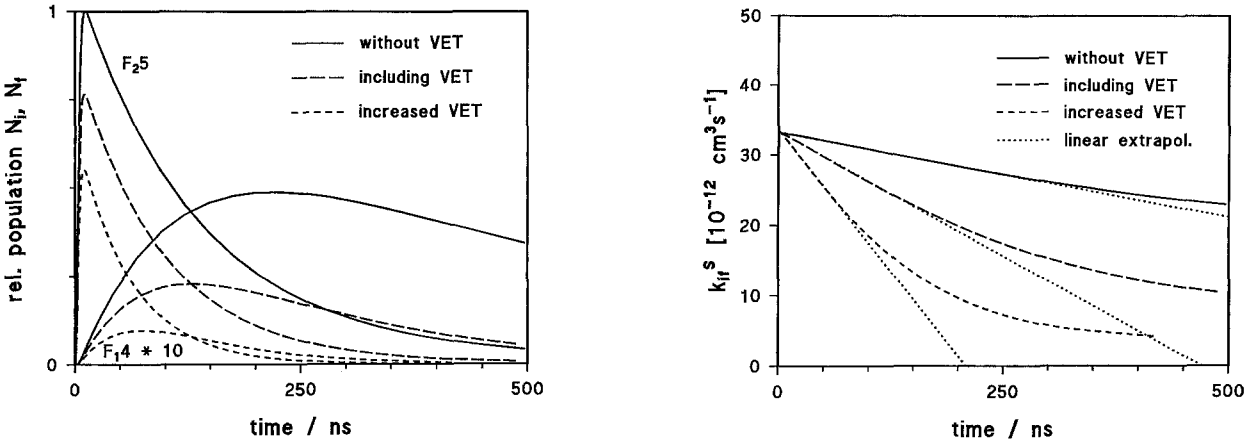

Fig. 1. Simulation of the rotational energy transfer from OH $(A, v' = 1)$ $F_2(5) \rightarrow F_1(4)$ by N_2 at 0.75 mbar and 300 K. *Solid lines*: without VET; *dashed lines*: including VET; *long dashes* (case **a**): VET as given by [13]; *short dashes* (case **b**): VET increased by a factor of 3; *left*: time-dependent populations, normalized to the maximum of the population in $F_2(5)$ without VET; *right*: time-dependent RET coefficients together with the linear extrapolation to $t = 0$

lated by RET is shown in the left panel of Fig. 1. The solid lines were obtained without VET, the dashed ones included VET. In case **a** (long dashes), the VET coefficients given in Table 2 were used; case **b** (short dashes) corresponds to an increase of the VET coefficients by a factor of 3, making VET the dominant loss term. The significant influence of VET on the time-dependent populations is obvious, and is even more pronounced for the collisionally populated level. The right panel in Fig. 1 shows, however, that in spite of the considerable differences in the populations, the RET coefficients determined from the extrapolation procedure is *exactly the same at time zero*. Again, the solid line corresponds to the case without, the broken ones to those with VET. The dotted lines – which exhibit quite different slopes – show the respective linear extrapolation of the time-dependent RET coefficient k_{if}^s. The true RET coefficient k_{if} for $F_2(5) \rightarrow F_1(4)$ transfer by N_2 at 300 K is given by the intercept at $t = t_0$ [(2); compare also Table 2]. Thus, the only effect of increasing vibrational energy transfer on the data evaluation procedure reported by Jörg et al. [1, 2] is the decrease of the time interval which can be used for a linear interpolation.

Figure 2 compares the calculated curves for case **a** (VET coefficients of [13]) with experimental data for the same initial and final levels. The measurements were performed in a collider mixture of equal mole fractions of N_2 and

Table 2. Parameters for the numerical model calculations presented in Figs. 1, 2. The RET behaviour upon excitation of the $(v' = 1)$ $F_2(5)$ state in N_2 at 0.75 mbar and 300 K was simulated. The corresponding coefficients for He are listed in brackets in order to facilitate a qualitative comparison of the calculation with experimental data in Fig. 2 which were taken in a He/N_2 mixture with a N_2 mole fraction of 0.5 at 1.5 mbar and 300 K

	$F_2(5)$	$F_1(4)$
Quenching coefficients [cm^3 s^{-1}], extrapolated from [13] (He: negligibly small [10])	2.5×10^{-11}	2.6×10^{-11}
VET coefficients [cm^3 s^{-1}], [13] (He: 1.3×10^{-12}, [10])	1.7×10^{-10}	1.7×10^{-10}
Total RET [cm^3 s^{-1}], ECS representation and extrapolation of the experimental data of this work[a] (He: estimate $\leq 7 \times 10^{-11}$, this work)	3.1×10^{-10}	4.3×10^{-10}
RET coefficient $F_2(5) \rightarrow F_1(4)$ [cm^3 s^{-1}], ECS representation of the experimental data of this work (He: 1.5×10^{-12}, this work)	3.3×10^{-11}	
Radiative decay rate [s^{-1}], [12, 13]	1.4×10^6	1.4×10^6
Total removal rate [s^{-1}], sum of quenching, VET, total RET and radiative decay		
without VET	7.5×10^6	9.7×10^6
with VET	10.6×10^6	12.8×10^6

[a] We would like to comment the striking level dependence obtained here by application of the ECS formalism; details of the ECS representation and extrapolation will be given in a future publication. In this work, state-to-state RET coefficients have been measured only for $[v' = 1, F_2(5)]$ excitation. A comparison with the data reported previously [2, 6] for $(v' = 0)$ and $F_2(5)$ and $F_2(4)$ excitation seems reasonable in view of the very similar RET behaviour for both vibrational levels. Since the dominant *individual* RET coefficients for transfer out of the $(v' = 0)$ and $F_2(5)$ state are, on average, more than 30% smaller than those for the corresponding transfer out of $(v' = 0)$ $F_2(4)$ [2, 6], a level dependence in the *total* RET coefficients of the order of 30% seems plausible, although no direct evidence is available for the $(v' = 1)$ $F_1(4)$ state

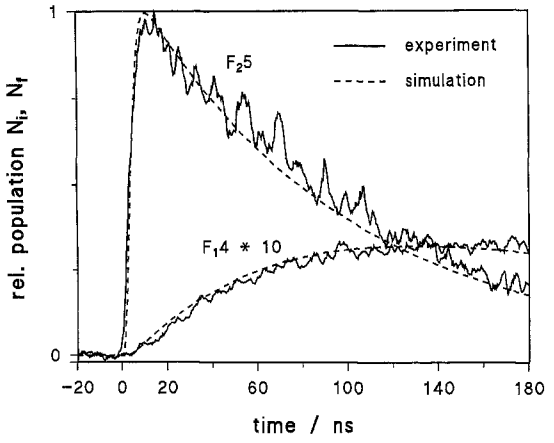

Fig. 2. Simulated time-dependent populations for case **a** in Fig. 1 together with experimental results in a mixture of equal mole fractions of He and N_2 at 1.5 mbar and 300 K, normalized to the maximum of the population in $F_2(5)$

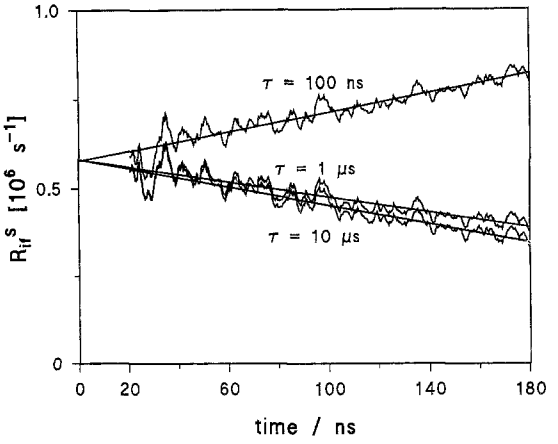

Fig. 3. Sensitivity of the evaluation of RET coefficients to variations in radiative lifetime; the same experimental data as in Fig. 2 were evaluated

He at 1.5 mbar and 300 K. Since our primary intention here is not a validation of the model calculation, but the proper consideration of the influence of VET in the data evaluation procedure, we regard, to a first approximation, experiment and simulation as equivalent for the following discussion, even though contributions by He to quenching, RET and VET were not included in the numerical model. Collisional energy transfer coefficients for He included in Table 2 show that this approximation seems quite appropriate for our purpose. The very good agreement of experiment and simulation demonstrated in Fig. 2 further supports our conclusion that RET coefficients may be evaluated using the formalism of Jörg et al. [1, 2] even in the presence of very efficient vibrational energy transfer.

2.3 Influence of Radiative Lifetime

According to (1), the radiative lifetime of the final state τ_f enters the data evaluation. Sensitivity to variations in τ_f are shown in Fig. 3. The same experimental data as shown in Fig. 2, measured at 300 K and 1.5 mbar in a collider mixture of He and N_2, were evaluated with $\tau_f = 1\,\mu s$, which is close to the radiative lifetime of about 750 ns reported in the literature [12, 13], as well as with $\tau_f = 100\,ns$ and $\tau_f = 10\,\mu s$. In contrast to Fig. 1, the quantity for which the extrapolation is performed is in this case a state-to-state RET rate R_{if}^s instead of a RET coefficient k_{if}^s because energy-transferring collisions of a gas *mixture* are considered (see below). The curves in Fig. 3 exhibit some interesting features. For radiative decay rates that are small compared to the collisional deactivation rates, the slopes of R_{if}^s versus time are almost identical and will approach a limiting value for even longer τ_f. Whereas the RET rate is underestimated in this case for increasing time, R_{if}^s is overpredicted for radiative decay rates which are higher than the deactivation rate of the collisionally populated state f. Most importantly, however, the extrapolated RET rate R_{if} at time zero is entirely independent of the state-specific radiative lifetime for this large range of τ_f. This behaviour was confirmed for different initial levels. Experimental uncertainties in the radiative lifetime thus have no effect on the measured RET coefficients or their accuracy [6]. For convenience, all data reduction was performed with $\tau_f = 1\,\mu s$.

2.4 Influence of Gas Composition and Pressure

In all RET experiments for Ar, N_2, CO_2, and H_2O, a background mole fraction of Helium had to be considered. (Small amounts of H_2, NO_2 or NO originating from the OH production process which could also be present in the observation volume were neglected in a first approximation; their potential influence on the measured RET coefficients will be discussed in the error analysis section.) Contributions to the energy transfer due to He were taken into account by considering the respective mole fractions and measured state-specific coefficients for RET caused by He. For example, the RET coefficient for N_2, k_{if,N_2}, is found by subtracting the He contribution, $k_{if,He} \times N_{He}$ from the extrapolated rate R_{if} at time zero

$$k_{if,N_2} = (R_{if} - k_{if,He} N_{He})/N_{N_2} \,. \tag{3}$$

The mole fraction of He was kept as low as possible. Typically, the fraction of the RET caused by He was 10–20% for H_2O; for the other colliders, RET by He amounted to 5–10% of the measured coefficient for collisional transfer leading to F_1 states and 20–30% for those transitions leading to F_2 levels (due to the propensity for $F_2 \rightarrow F_2$ conservation in collisions with He). For all colliders, the total pressure in the discharge flow reactor was varied by about a factor of 3 (see Table 1); in none of the experiments, a dependence of the RET coefficient on pressure was observed.

3 Results and Discussion

The measured state-to-state RET coefficients for thermal collisions of OH in the ($A^2\Sigma^+$, $v' = 1$) state are listed in Table 3; statistical errors are given as one standard deviation. Figures 4–8 show the RET coefficients in comparison with

[6] For a detailed discussion, we refer to Jörg et al. [1]

Table 3. RET coefficients ($k/10^{-12}\,cm^3\,s^{-1}$) for thermal collisions of OH [$A^2\Sigma^+$, $v' = 1$, $F_2(5)$]

	He	Ar	N_2	CO_2	H_2O
$F_1(6)$	0.7 ± 0.2	8.0 ± 1.0	12 ± 1.2	13 ± 1.3	15 ± 4
$F_2(6)$	8.8 ± 0.7	13 ± 1.3	26 ± 2.4	16 ± 2.0	180 ± 36
$F_1(5)$	5.9 ± 0.5	78 ± 6.2	46 ± 4.5	71 ± 5.7	46 ± 9
$F_2(5)$	Excited state				
$F_1(4)$	2.5 ± 0.3	19 ± 2.5	29 ± 2.3	24 ± 3.0	47 ± 9
$F_2(4)$	14.6 ± 1.4	33 ± 2.6	63 ± 5.2	26 ± 2.6	460 ± 100
$F_1(3)$	3.4 ± 0.4	16 ± 1.8	22 ± 2.1	14 ± 4.2	51 ± 13
$F_2(3)$	13.8 ± 1.0	19 ± 2.4	32 ± 4.5	19 ± 5.7	150 ± 30
$F_1(2)$	2.6 ± 0.3	7.8 ± 1.2			31 ± 10
$F_2(2)$	4.2 ± 0.4	9.6 ± 1.4			96 ± 30

those measured before for $v' = 0$ [1, 2, 6]. In all cases, the excited rotational/fine structure level is $F_2(5)$. The upper panels of Figs. 4–8 contain the measured RET coefficients for $F_2 \rightarrow F_2$ transitions, the lower ones those for $F_2 \rightarrow F_1$ transitions. Due to experimental limitations, the entire matrix of transitions to final states with $N' = 0$–6 could not be measured for $v' = 1$, however, this does not preclude a comparative discussion of the RET behaviour observed for both vibrational states [7]. In general, the RET in $v' = 1$ and $v' = 0$ is strikingly similar in both qualitative trends as well as magnitude of individual coefficients. Propensities for symmetry conservations are largely the same as reported before for RET in the $v' = 0$ state [1, 2, 6].

3.1 RET *by Helium*

For Helium as collision partner, a strong propensity for symmetry conservation is observed in $v' = 1$ (Fig. 4). By far the strongest transitions are those to the $F_2(4)$ and $F_2(3)$ states. However, the variation with even versus odd $\Delta N'$ seems to be less pronounced for the excited vibrational level than for $v' = 0$ [1, 2]. Quantum scattering calculations for RET in OH ($A, v' = 0$) by He [3] attributed this behaviour to the highly symmetric OH (A)–He interaction potential. Thus, one might argue that for $v' = 1$, the potential energy surface might be less symmetric. However, this is only speculation, since it is not possible to infer the shape of the interaction potential from our experimental data.

3.2 RET *by Argon*

RET of OH ($A^2\Sigma^+$, $v' = 1$) with Argon as collision partner shows almost identical probabilities for $F_2 \rightarrow F_1$ and $F_2 \rightarrow F_2$ transfer (Fig. 5). The largest coefficient is that for the nearly isoenergetic $F_2(5) \rightarrow F_1(5)$ transition. Within the experimental error limits, the RET coefficients for the $v' = 1$ state are in general the same as those for $v' = 0$, with the most obvious exception being that for $F_2(5) \rightarrow F_1(5)$ transfer. It should be pointed out, however,

[7] If no coefficient is given for a specific final state, this does not imply the coefficient to be zero – instead, it means that the corresponding transition was not accessible in our experiments

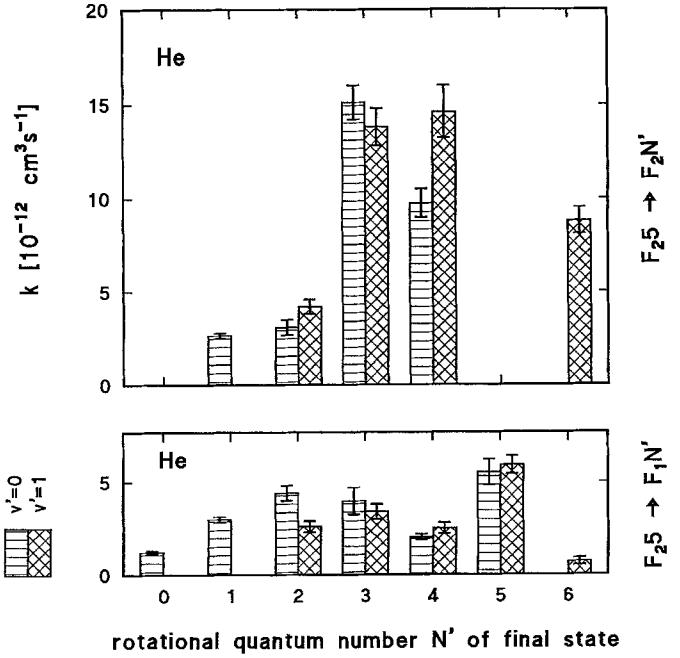

Fig. 4. State-to-state RET coefficients for thermal collisions of OH ($A, v' = 1$) with He[7]. The $F_2(5)$ level was excited. Data obtained previously [1, 2] for the same initial level in the $v' = 0$ state are included for comparison

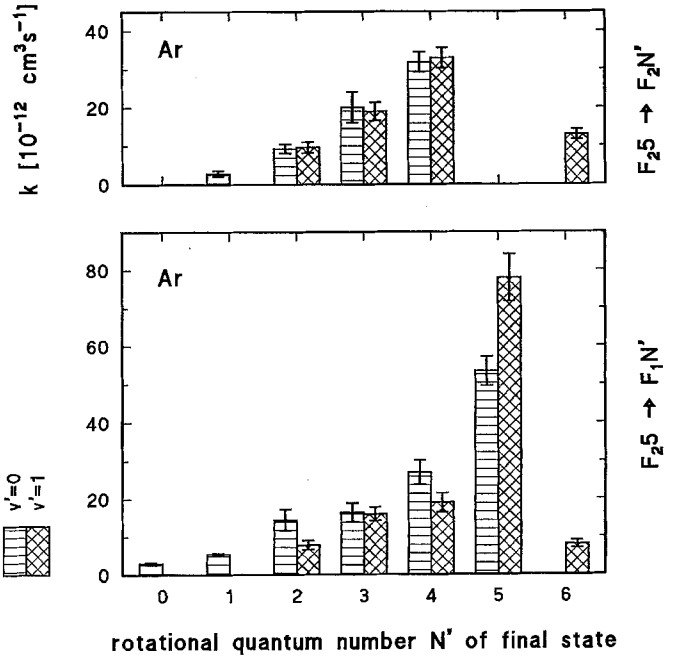

Fig. 5. State-to-state RET coefficients for thermal collisions of OH ($A, v' = 1$) with OH[7]. The $F_2(5)$ level was excited. Data obtained previously [1, 2] for the same initial level in the $v' = 0$ state are included for comparison

that this coefficient was determined directly from time-resolved fluorescence measurements for $v' = 1$ whereas it had to be evaluated from fluorescence spectra for the $v' = 0$ state; the latter method is less suited to quantify contributions of multiple collisions and thus suffers from inherently larger systematic errors [1].

3.3 RET *by* N_2

As observed before for the $v' = 0$ state, RET of OH ($A^2\Sigma^+$) by N_2 (Fig. 6) exhibits a moderate tendency for symmetry conservation [6]. The largest coefficient is that for the $F_2(5) \rightarrow F_2(4)$ transition. The RET coefficients for transfer from $F_2(5)$ to $F_1(2)$ and to $F_2(2)$ could not be obtained for the following reasons. The $R_2(1)$ line in the $(1,1)$ band at 314.07 nm, which was used to detect fluorescence from the $F_2(2)$ state, overlaps with the $(0,0)$ $P_2(11)$ line. Similary, the $Q_1(2,2')$ structure in the $(1,1)$ band at about 313.62 nm, which was used to monitor the fluorescence from the $F_1(2)$ state, it located near the $(0,0)$ $P_1(11)$ line at 313.69 nm. Due to fast VET [11, 13] induced by collisions of OH ($A^2\Sigma^+$) with N_2, the fluorescence of the neighbouring lines in the $(0,0)$ band was strong enough to preclude measurements of both RET coefficients mentioned above. This was not a problem in the RET measurements for OH ($A^2\Sigma^+$, $v' = 1$) with He and Ar, where total RET from one initial level is much larger than total VET [10, 15].

3.4 RET *by* CO_2

For CO_2 as collision partner the RET exhibits a behaviour similar to that of Ar (Fig. 7), the same effect which has been observed in the $v' = 0$ state [6]. The largest individual RET coefficient is that for the almost isoenergetic transition $F_2(5) \rightarrow F_1(5)$. On average, the coefficients are about 35% smaller than the corresponding ones for $v' = 0$. For the same reason as in the experiments with N_2, transfer to $F_1(2)$ and $F_2(2)$ could not be measured; fast VET by CO_2 [11] leads to significant fluorescence of the $(0,0)$ $P_1(11)$ and $P_2(11)$ lines which interferes with the detection of $(1,1)$ $R_2(1)$ and $Q_1(2,2')$. Although state-specific VET was not investigated in this work, a few conclusions on the VET behaviour of N_2 and CO_2 may be drawn from time-resolved fluorescence spectra measured upon excitation of $v' = 1$, $F_2(5)$. In agreement with previous observations [10, 15], we have no evidence for strong VET between almost isoenergetic levels (as from $v' = 1$, $N' = 5$ to $v' = 0$, $N' = 14$). It seems, however, that predominantly the higher rotational levels ($N' > 10$) in the $v' = 0$ state are populated by VET from $F_2(5)$; this is in qualitative accord with the observation [10] of rotationally hot distributions in $v' = 0$ after collisions of OH ($A^2\Sigma^+$, $v' = 1$, $N' = 0, 3, 5$) with N_2.

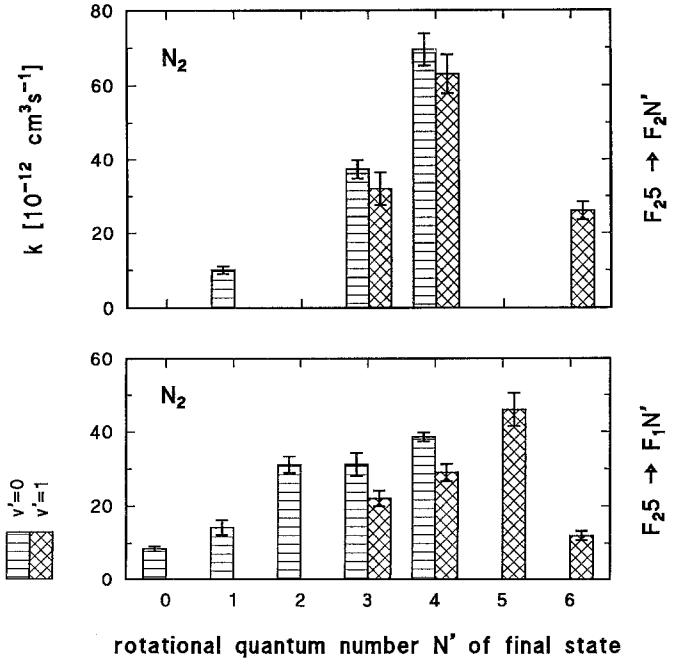

Fig. 6. State-to-state RET coefficients for thermal collisions of OH ($A, v' = 1$) with N_2 [7]. The $F_2(5)$ level was excited. Data obtained previously [2, 6] for the same initial level in the $v' = 0$ state are included for comparison

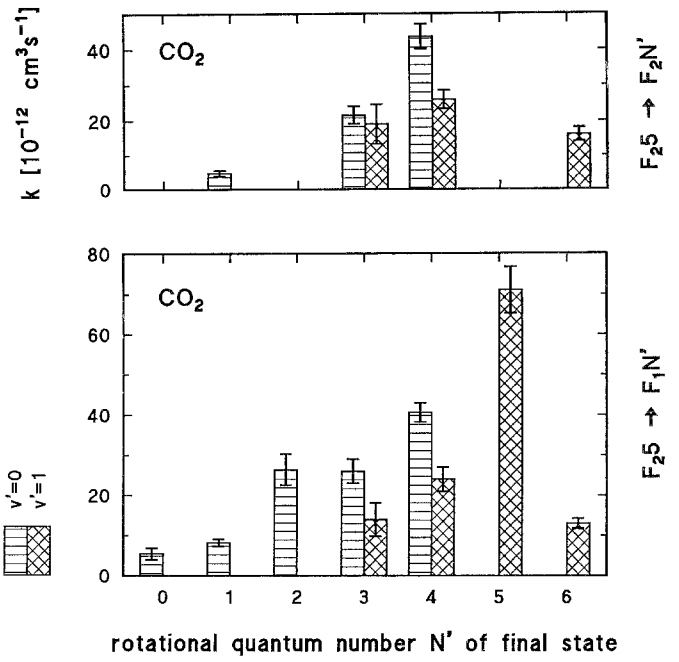

Fig. 7. State-to-state RET coefficients for thermal collisions of OH ($A, v' = 1$) with CO_2 [7]. The $F_2(5)$ level was excited. Data obtained previously [2, 6] for the same initial level in the $v' = 0$ state are included for comparison

3.5 RET *by* H_2O

RET in OH ($A^2\Sigma^+$, $v' = 1$) with H_2O as collision partner shows a high propensity for symmetry conservation (Fig. 8). Again, the qualitative behaviour is very similar to that observed for $v' = 0$. By far the largest coefficient is that for $F_2(5) \rightarrow F_2(4)$ transfer; it is about an order of magnitude larger than the corresponding one for symmetry-changing collisions, $F_2(5) \rightarrow F_1(4)$. On average, the individual RET coefficients are about 25% larger than those for $v' = 0$. VET by H_2O is inefficient [11]; interferences by lines in the $(0,0)$ band were not observed in the fluorescence spectra.

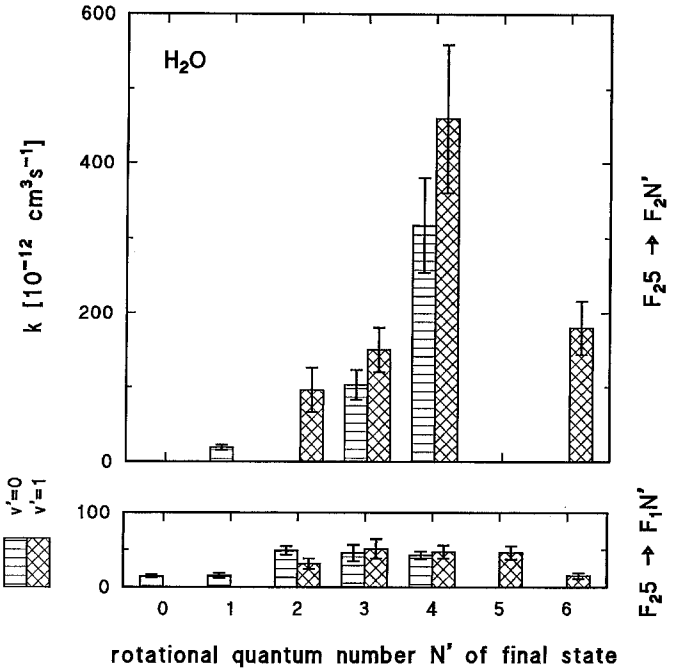

Fig. 8. State-to-state RET coefficients for thermal collisions of OH ($A, v' = 1$) with H_2O[7]. The $F_2(5)$ level was excited. Data obtained previously [2, 6] for the same initial level in the $v' = 0$ state are included for comparison

3.6 Total RET

A direct comparison of the measured RET coefficients of this work with literature values – apart from that with the data of Jörg et al. [1, 6] for $v' = 0$ – is not possible, since investigations of the *state-to-state RET* in OH ($A^2\Sigma^+$, $v' = 1$) are lacking. However, Burris et al. [13, 16] have measured total removal (the sum of quenching, VET and RET) by N_2 for different excited levels in OH ($A^2\Sigma^+$, $v' = 0$ and $v' = 1$) and deduced *total RET coefficients* for specific excited levels from their measurements. It should be pointed out that their total RET rates (for excitation of a single rotational level) are determined from the rates for total decay of single-line fluorescence (originating from the laser-excited levels) reduced by the quenching and VET rates – a procedure which leads to comparatively large errors. Burris et al. [13] report total RET coefficients for collisions of OH (A) with N_2 of between $2.1 \times 10^{-10}\,cm^3\,s^{-1}$ and $3.1 \times 10^{-10}\,cm^3\,s^{-1}$ for excitation of $v' = 1$, $0 \leq N' \leq 4$; considering the statistical errors no systematic trend is discernible for this range. The same authors give a total RET coefficient of $3.0 \times 10^{-10}\,cm^3\,s^{-1}$, which is almost independent of rotational level for excitation of $v' = 0$, $1 \leq N' \leq 4$ [16]. Although total RET upon $N' = 5$ excitation was not measured, average values of $(2.7 \pm 0.4) \times 10^{-10}\,cm^3\,s^{-1}$ for $v' = 1$, $N' = 5$ and $(3.0 \pm 0.2) \times 10^{-10}\,cm^3\,s^{-1}$ for $v' = 0$, $N' = 5$ seem realistic from extrapolation of their data. Lengel and Crosley [17] report $4.1 \times 10^{-10}\,cm^3\,s^{-1}$ for total RET by N_2 out of $v' = 0$, $N' = 4$ and $N' = 6$. We can estimate total RET coefficients from the sum of our measured state-to-state coefficients. For excitation of $v' = 0$, $F_2(4)$, $v' = 0$, $F_2(5)$ and $v' = 1$, $F_2(5)$, we thus obtain $(5.4 \pm 0.5) \times 10^{-10}\,cm^3\,s^{-1}$, $(3.8 \pm 0.4) \times 10^{-10}\,cm^3\,s^{-1}$ and $(3.2 \pm 0.3) \times 10^{-10}\,cm^3\,s^{-1}$, respectively. In view of the error limits of the different measurements, these values are in satisfactory agreement.

Table 4. Total RET coefficients ($k_{tot}/10^{-11}\,cm^3\,s^{-1}$) at 300 K for inelastic collisions of OH ($A^2\Sigma^+$) with He, Ar, N_2, CO_2, and H_2O following excitation of the $F_2(5)$ levels in both $v' = 0$ and $v' = 1$

Collider	k_{tot} in $v' = 1$		k_{tot} in $v' = 0$	
He	6.6		6.0 [1]	
Ar	22		21 [1]	
N_2	32	27 [13]	38 [6]	30 [16]
				41 [17]
CO_2	22		35 [6]	
H_2O	117		91 [6]	

This work: k_{tot} is the sum of all individual RET coefficients k_{if} with i = $F_2(5)$; missing state-to-state coefficients were estimated, using analogies of the RET for the two vibrational states
[1, 6]: estimated from measured state-to-state coefficients as in this work
[13]: extrapolated from coefficients given for $0 \leq N' \leq 4$
[16]: level-independent coefficients given for $0 \leq N' \leq 4$
[17]: identical coefficient for $N' = 4$ and 6

Motivated by the lack of experimental data, we similarly attempted to provide an estimate of the magnitude of total RET coefficients for all other colliders. Directly measured state-to-state coefficients were added, and those not accessible to our measurements were estimated using similarities observed in the RET for the two vibrational states. Table 4 shows the results together with the available literature data on room temperature RET. Total RET by He is much smaller than by all other collisions partners. Not surprisingly, total RET by H_2O is very efficient. For N_2, Ar and CO_2, the estimated total RET coefficients are of the same magnitude. Comparing the total RET coefficients for the two different vibrational levels, $v' = 0$ and $v' = 1$, they are indistinguishable within the error bars for He and Ar. Those for N_2, H_2O and CO_2 exhibit differences for $v' = 0$ compared with $v' = 1$ excitation on the order of 15%, 25% and 45%, respectively. It can thus be concluded that for the same initial rotational level in both vibrational states, the total RET coefficients are all of very similar magnitude.

4 Analysis of Statistical and Systematic Errors

Regarding the state-to-state RET coefficients for collisions of OH ($A^2\Sigma^+$, $v' = 1$) with the different colliders investigated in this work and comparing them to the values determined previously for OH ($A^2\Sigma^+$, $v' = 0$) [1, 2, 6], the question arises as to which of the small differences we have observed are physically significant. Therefore an evaluation of potential error sources is necessary. Errors may stem from the experiment itself (e.g., fluctuations in laser wavelength or in the gas flows) or from the data evaluation (e.g., corrections for the influence of "background" colliders as He, H_2, NO, or NO_2).

4.1 Measurement of Time-Dependent Fluorescence Signals

There are several parameters which could influence the accuracy of the determination of the time-dependent fluorescence signals. In a typical measurement, the fluorescence

signal of the $R_2(4)$ line (which serves as a monitor for the laser-coupled state) is measured several times, and the signal corresponding to teach particular final state populated by collisions is measured once. Fluctuations in laser intensity, laser wavelength and OH production affect the broad-band reference channel in the same way as the spectrally resolved time-dependent signals. Thus, a normalization of the actual measurement by the reference signal eliminates the influence of these fluctuations. The changes in the reference signal were typically on the order of 2–5%; series with variations of more than 10% ion the reference signal were not evaluated. All fluorescence intensities were measured at fixed wavelength position which may, in principle, be affected by drifts in the monochromator wavelength calibration (e.g., due to small variations in room temperature). Therefore, the line positions were checked at the beginning of every day. Typically, deviations were less than 0.01 nm (at the $R_2(4)$ peak) **before** a new wavelength calibration; this corresponds to changes of 10–20% in fluorescence intensity. Wavelength drifts **within** one series of measurements are less than this upper limit, because the peak intensity of the $R_2(4)$ line typically changed by 5–10% during one set of experiments. The uncertainty in the line position is a random error and thus tends to diminish with increasing numbers of measured series.

4.2 Evaluation Procedure

The conversion of fluorescence intensities to number densities relies on tabulated isotropic Einstein coefficients [9] and requires that any orientational preference of the fluorescence (e.g., due to polarization of the laser light) is negligible. Therefore we used a polarization scrambler in the exciting beam. By comparing the ratios of fluorescence intensities of all the lines originating from a single excited level with the isotropic Einstein coefficients we could check for any residual polarization in the fluorescence signals. An example for this type of measurement is given in [1]. Polarization was negligible in all experiments.

Additional minor error sources in the data analysis are the choice of t_0, which corresponds to the starting time of the laser pulse, as well as of the time interval used for the extrapolation. By systematic variation of these parameters for typical data traces, their influence on the RET coefficients was found to be less than 5%.

4.3 Influence of Gas Composition

The gas composition can influence the accuracy of the measured RET coefficients in several ways. The most obvious source of error is an uncertainty in the collider flow. If the contribution of He [see (3)] to the RET rate is small, the error in the RET coefficient is proportional to the error in the collider mole fraction. Any systematic deviation in the calibration of the flow meters would affect an entire set of RET coefficients for a given collider and would not change the ratios of coefficients within the RET matrix. We have therefore regularly checked the calibration of the flow meters; typically, the accuracy of the measured flows is 2–3% with the exception of H_2O. Due to the tendency of H_2O to condense in tubings and in the flow meter itself, the errors were of the order of 20%, despite of moderately heating the entire gas inlet system.

Uncertainties in the RET coefficients of the buffer gas He have a negligible influence on the evaluation. Although the He mole fraction was quite large in some cases, the fraction of the RET caused by He was below 30%, typically 10–20% due to the very small RET coefficients of He in comparison to the other colliders. This fraction was subtracted as described in Sect. 2.4; errors in the He flow affected the RET coefficients by less than 1%.

The presence of H_2, NO_2 and NO – which are involved in the OH production – was neglected in the data evaluation. With an estimate of $k_{\mathrm{if},H_2} \approx 0.5 k_{\mathrm{if},N_2}$ [17] and $k_{\mathrm{if,NO}} \approx k_{\mathrm{if},NO_2} \approx k_{\mathrm{if},N_2}$, the influence of these colliders was calculated to be negligible (<3%) for RET measurements with N_2, CO_2 and H_2. The error due to this background quenching was in general less than 5% for the measurements with Ar and He. Only the smallest RET coefficients for collisions with He may be overestimated by approximately 10%.

4.4 Reproducibility

The reproducibility of the results, involving repeated calibration procedures as well as changes in experimental setup and equipment, gives the best impression of the overall accuracy of the measured RET coefficients. For He, Ar, N_2, and CO_2, the coefficients could be reproduced within 10–15% within a period of several months, even after completely removing and reassembling the apparatus due to construction work in the laboratory building. However for H_2O, variations in the RET coefficients by 20–30% were observed for different series. Similarly, calibrations of the H_2O flow meter by different experimentors at various times exhibited differences of up to 25%; these fluctuations, which could not easily be controlled and which are most probably caused by partial water condensation, are responsible for the larger errors in the RET measurements with H_2O. We thus attribute an average error of 15% to the RET coefficients for collisions of OH ($A^2\Sigma^+$, $v' = 1$) with He, Ar, N_2, and CO_2 and of 30% for those with H_2O. With respect to these error limits, we judge the RET coefficients for He, Ar and N_2 to be identical for the same initial rotational/fine structure level in both vibrational states, whereas the differences for CO_2 seem to be significant. For H_2O as collision partner, a higher accuracy would be desirable to decide whether the RET coefficients are different for the two vibrational states.

5 Summary and Perspectives

We have, for the first time, measured state-to-state rotational energy transfer coefficients for thermal collisions of OH ($A^2\Sigma^+$, $v' = 1$) at 300 K; energy transfer by He, Ar, N_2, CO_2, and H_2O was investigated. The results are strikingly similar to those obtained before in a study on RET in OH ($A^2\Sigma^+$, $v' = 0$) [1, 2, 6]. These observations might give, in an indirect way, some clues on the interaction potentials which might not be greatly deformed upon addition of one

vibrational quantum to the energy of the OH (A) state. It would be very interesting to compare the results with ab initio calculations wherever feasible. Since common OH laser-induced fluorescence schemes for the measurement of OH concentration and temperature often employ $v' = 1$ excitation, the reported RET coefficients are furthermore valuable in the quantitative interpretation of such measurements. We are currently attempting to represent the measured coefficients by simple relations which can be incorporated in a dynamic model of OH LIF. This model will be used to systematically analyze the potential of different LIF measurement strategies. For application of such a model in combustion studies, RET data at flame temperatures are required. Recent quantum scattering calculations [3–5] for collisions of OH ($A, v' = 0$) with He and Ar – which agree very well with our measured data – provide a valuable basis for extensions of the data to higher temperatures. First results for the scaling of our measured RET coefficients for H_2O to flame temperatures by an approach based upon the IOS scaling law for $^2\Sigma^+$ states [14] are promising: the agreement of measured and simulated spectra in H_2/O_2 low-pressure flames with H_2O as the dominant collider is very satisfactory. Measurements of level-dependent total RET and electronic quenching at flame temperature are currently being performed in order to extend the data base necessary for the detailed simulation of all radiative and collisional processes in OH LIF.

Acknowledgements. We gratefully acknowledge support of this work by the German Ministry of Research and Technology (BMFT) within the research program TECLFAM.

References

1. A. Jörg, U. Meier, K. Kohse-Höinghaus: J. Chem. Phys. **93**, 6453 (1990)
2. A. Jörg: Dissertation, DLR Stuttgart/Universität Bielefeld (1991)
3. A. Jörg, A. Degli Esposti, H.-J. Werner: J. Chem. Phys. **93**, 8757 (1990)
4. A. Degli Esposti, H.-J. Werner: J. Chem. Phys. **93**, 3351 (1990)
5. M.H. Alexander, A. Berning, A. Degli Esposti, A. Jörg, A. Kliesch, H.-J. Werner: Ber. Bunsenges. **94**, 1253 (1990)
6. A. Jörg, U. Meier, R. Kienle, K. Kohse-Höinghaus: Appl. Phys. B **55**, 305 (1992)
7. G.H. Dieke, H.M. Crosswhite: J. Quant. Spectrosc. Radiat. Transfer **2**, 97 (1962)
8. M.H. Alexander, J.E. Smedley, G.C. Corey: J. Chem. Phys. **84**, 3049 (1986)
9. M.R. Trolier: Ph.D. Thesis, Cornell University, 1988
10. R.K. Lengel, D.R. Cosley: J. Chem. Phys. **68**, 5309 (1978)
11. R.A. Copeland, M.L. Wise, D.R. Crosley: J. Phys. Chem. **92**, 5710 (1988)
12. P. Hogan, D.D. Davis: Chem. Phys. Lett. **92**, 555 (1974)
13. J. Burris, J.J. Butler, T.J. McGee, W.S. Heaps: Chem. Phys. **124**, 251 (1988)
14. M.H. Alexander: J. Chem. Phys. **76**, 3637 (1982)
15. R.K. Lengel, D.R. Crosley: Chem. Phys. Lett. **32**, 261 (1975)
16. J. Burris, J. Butler, T. McGee, W. Heaps: Chem. Phys. **151**, 233 (1991)
17. R.K. Lengel, D.R. Crosley: J. Chem. Phys. **67**, 2085 (1977)